Title

Detection and Quantification of GPCR mRNA: An Assessment and Implications of Data from High-Content Methods

Journal

ACS Omega, 4(16)

ISSN

2470-1343

Authors

Sriram, Krishna
Wiley, Shu Z
Moyung, Kevin
et al.

Publication Date

2019-10-15

DOI

10.1021/acsomega.9b02811

Peer reviewed

ACS OMEGA

Article

Cite This: ACS Omega 2019, 4, 17048−17059

http://pubs.acs.org/journal/acsodf

Detection and Quantification of GPCR mRNA: An Assessment and Implications of Data from High-Content Methods

Krishna Sriram,[†] Shu Z. Wiley,[†] Kevin Moyung,[†] Matthew W. Gorr,[†] Cristina Salmerón,[†] Jordin Marucut,[†] Randall P. French,[‡,§] Andrew M. Lowy,[‡,§] and Paul A. Insel*[,†,∥]

[†]Department of Pharmacology, [‡]Department of Surgery, [§]Moores Cancer Center, and [∥]Department of Medicine, University of California, San Diego, La Jolla, California 92093-0636, United States

Supporting Information

ABSTRACT: G protein-coupled receptors (GPCRs) are the largest family of membrane receptors and targets for approved drugs. The analysis of GPCR expression is, thus, important for drug discovery and typically involves messenger RNA (mRNA)-based methods. We compared transcriptomic complementary DNA (cDNA) (Affymetrix) microarrays, RNA sequencing (RNA-seq), and quantitative polymerase chain reaction (qPCR)-based TaqMan arrays for their ability to detect and quantify expression of endoGPCRs (nonchemosensory GPCRs with endogenous agonists). In human pancreatic cancer-associated fibroblasts, RNA-seq and TaqMan arrays yielded closely correlated values for GPCR number (∼100) and expression levels, as validated by independent qPCR. By contrast, the microarrays failed to identify ∼30 such GPCRs and generated data poorly correlated with results from those methods. RNA-seq and TaqMan arrays also yielded comparable results for GPCRs in human cardiac fibroblasts, pancreatic stellate cells, cancer cell lines, and pulmonary arterial smooth muscle cells. The magnitude of mRNA expression for several Gq/11-coupled GPCRs predicted cytosolic calcium increase and cell migration by cognate agonists. RNA-seq also revealed splice variants for endoGPCRs. Thus, RNA-seq and qPCR-based arrays are much better suited than transcriptomic cDNA microarrays for assessing GPCR expression and can yield results predictive of functional responses, findings that have implications for GPCR biology and drug discovery.

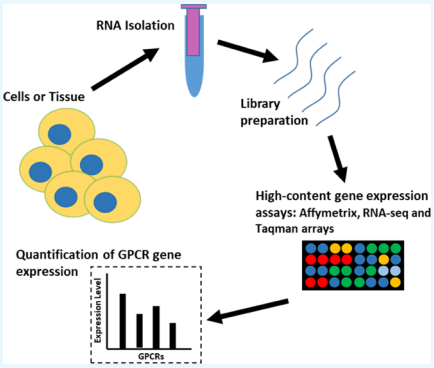

INTRODUCTION

G protein-coupled receptors (GPCRs), a family of >800 membrane proteins in humans, respond to a wide range of peptides, proteins, lipids, metabolites, etc. and regulate a broad range of cellular processes including proliferation, metabolism, and protein synthesis. There are ∼360 GPCRs that are activated by endogenous agonists, i.e., endoGPCRs other than visual, taste, and olfactory receptors. EndoGPCRs are targets for a large fraction (∼35%) of approved drugs.[1] The detection of GPCRs in cells and tissues is, thus, valuable for identifying GPCRs and defining their roles in cell physiology and pathophysiology as well as for identifying opportunities for drug discovery.

The detection of GPCRs by protein-based methods is challenging. Due to their low expression, GPCRs are difficult to assay by current proteomic methods, plus the paucity of well-validated antibodies for many GPCRs makes it problematic to detect them by immunological techniques. As a consequence, the detection of GPCRs, especially in efforts to profile their expression in cells and tissues, relies on assays of messenger RNA (mRNA) expression. Multiple methods can assess mRNA expression but their utility for defining GPCR expression has not been assessed. We, thus, sought to evaluate GPCR expression by parallel analysis of RNA samples from a single-cell-type: human pancreatic cancer-associated fibroblasts (CAFs) tested with three different techniques: TaqMan arrays, RNA sequencing (RNA-seq), and transcriptomic complementary DNA (cDNA) [e.g., Affymetrix (Affy)] arrays. Due to the low expression of most GPCRs, even at the mRNA level, such a comparison is important for evaluating data in public databases (e.g., CCLE[2]) that were generated using transcriptomic (Affymetrix) arrays. Because of the limited dynamic range of such arrays, it is unclear if that approach reveals accurate data regarding GPCRs. We show here that Affymetrix arrays detect fewer GPCRs than either TaqMan arrays or RNA-seq but that results from the latter two methods agree closely in terms of identity and magnitude of GPCR expression. We also provide independent quantitative polymerase chain reaction (qPCR) validation of GPCR expression data from TaqMan arrays and RNA-seq and evidence for the predictive value of data from the latter techniques in terms of signaling and physiological response of Gq/11-coupled GPCRs.

Here, we assess GPCR expression data for the following human cells and tissues: (1) pancreatic CAFs (using Affymetrix HG U133plus2.0 arrays, TaqMan arrays, and

Received: August 30, 2019
Accepted: September 12, 2019
Published: September 30, 2019

DOI: 10.1021/acsomega.9b02811
ACS Omega 2019, 4, 17048−17059

RNA-seq); (2) cardiac fibroblasts (CFs), pulmonary arterial smooth muscle cells (PASMCs), and pancreatic stellate cells (PSCs) (using TaqMan arrays and RNA-seq); (3) AsPC-1 pancreatic cancer cell line (from CCLE, via Affymetrix HG U133plus2.0 plus RNA-seq and via TaqMan arrays in our laboratory); (4) MDA-MB-231 breast cancer cell line (from CCLE via Affymetrix HG U133plus2.0 and RNA-seq); (5) ovarian cancer (OV) tissue and lung squamous cell carcinoma (LUSC) tissue (from TCGA, via Affymetrix HG U133a and RNA-seq). This large number of sample types (also listed in Table S1), with data collected from different sources, facilitated a robust comparison of GPCR detection and revealed prominent differences in data generated by the different methods. These findings provide insights regarding GPCR expression by various cell types, a rationale for the interpretation of mined data regarding GPCR expression, and evidence for the utility of mRNA expression data in predicting the functional activity of one class of GPCRs (Gq/11-coupled GPCRs). Together such information should aid studies of GPCR biology and drug discovery.

METHODS

Cell Culture and RNA Isolation. CAFs were isolated from primary human PDAC tumors via explant and were grown, as described previously.[3] At low passage (<5), CAFs were plated in 10 cm plates and grown in 5% CO_2 at 37 °C. Cells were lysed and RNA was isolated using a Qiagen RNeasy kit (Cat # 74104, Qiagen, Hilden, Germany), with on-column DNase-1 digestion (79254, Qiagen). Purified RNA had 260/280 ratios ~2 (via Nanodrop 2000c, ThermoFischer Scientific, Waltham, MA) and RNA integrity number scores >9 (via Bioanalyzer, Agilent Technologies, Santa Clara, CA). Human fetal cardiac fibroblasts (CFs) were obtained from Cell Biologics, Cat # H6049 (Chicago, IL) and grown in 10% CO_2 at 37 °C, in low-glucose Dulbecco's modified Eagle's medium (DMEM) (Cat # D60646 Gibco, Dublin, Ireland) with 2% fetal bovine serum (FBS) (Cat # FB-02, Omega Scientific Inc., Tarzana, CA), 5 μg/L of FGF2 (Cat # 130093838, Miltenyi Biotec, San Diego, CA), 5 mg/L of insulin (Cat # SC360248, Santa Cruz Biotechnology, Dallas, TX), 1 mg/L of hydrocortisone hemisuccinate (Cat # 07904, Stemcell Technologies Inc., Cambridge, MA), and 50 mg/L of ascorbic acid (Cat # A454425G, Sigma-Aldrich, St. Louis, MO). Pulmonary arterial smooth muscle cells (PASMCs) were obtained from Lonza (Cat # CC-2581, Walkersville, MD) and were cultured in 5% CO_2 at 37 °C in low-glucose DMEM with 5% FBS, epidermal growth factor (5 ng/mL), FGF2 (5 ng/mL, Cat # 130093837, Miltenyi Biotec), insulin (same as above), and ascorbic acid (50 μg/mL). Pancreatic stellate cells (PSCs) were purchased from ScienCell Research Laboratories (Cat # 3830; ScienCell Research Laboratories, Carlsbad, CA) and cultured according to the manufacturers' instructions.

qPCR. RNAs were converted to cDNA via the Superscript III kit (Cat # 18080050, Thermo Fisher Scientific, Waltham, MA). cDNA was then mixed with gene-specific primers (2 μM) and Perfecta SYBR green SuperMix reagent (Cat # MP9505402K, VWR, Radnor, PA) for PCR amplification using a DNA Engine Opticon 2 system (MJ Research, St. Bruno, QC, Canada). Primers were designed using the Primer3Plus software. The primer sequences are listed in Table S3.

RNA-seq. RNA sequencing was performed by DNAlink Inc. (San Diego, CA for CAF samples) or the UCSD IGM core (for CF and PASMC samples), using TruSeq (Illumina, San Diego, CA) stranded mRNA library preparation, with sequencing on a Nextera 500 (for CAF samples) or a HiSeq 4000 (CF and PASMC samples) at 50 (CFs and PASMCs) or 75 (CAFs) base-pair single reads. Data were analyzed via Kallisto v0.43.1[4] using the Ensembl GRCh38 v79 reference transcriptome, with 100 bootstraps, to obtain transcript-level expression in transcripts per million (TPM). Kallisto bootstraps were read in R via Sleuth;[5] GPCR data for each bootstrap were evaluated as described below to quantify the uncertainty of GPCR expression quantification. Gene-level expression in TPM was calculated using Tximport.[6] For the comparison of expression ratios of gene expression between samples, gene-level estimated counts data from tximport were input into edgeR,[7] to obtain normalized gene expression in counts per million (CPM). RNA-seq raw data are available at National Center for Biotechnology Information Gene Expression Omnibus (NCBI GEO), at accession numbers GSE101665 and GSE125049.

TaqMan Arrays. cDNA was diluted with double-distilled H_2O and mixed with TaqMan Universal PCR Master Mix (Cat # 4304437, Life Technologies, Waltham, MA) to a final concentration of 1 mg/mL and assayed for GPCR expression using TaqMan GPCR arrays (Cat # 4367785; Life Technologies) by a 7900HT fast real-time system (Thermo Fisher Scientific). Data were analyzed with the RQ Manager software (Life Technologies). Gene expression was normalized to that of 18 S ribosomal RNA as ΔCt; the results were consistent if normalized to glyceraldehyde 3-phosphate dehydrogenase (GAPDH) or other housekeeping genes;[8] based on previous studies, we set the TaqMan GPCR array detection threshold to a ΔCt value (relative to 18 S) ≤25.[3,8,9]

Affymetrix Arrays. RNA samples were submitted to the Technology Center for Genomics & Bioinformatics at UCLA for analysis via Affymetrix HG U133plus2.0 arrays. Data as cel files were analyzed by both the MAS5 and RMA methods to quantify gene expression. The analysis was performed via the R "affy" package[10] to yield intensity estimates for each probe set, along with detection *p*-values and present/absent calls (for the MAS5 method). For a GPCR to be considered "detected" in Results section, the Mas5 call was required to indicate present ("P") for at least one probe set for a given gene. In the event that multiple different probe sets for the same GPCR indicated a P call (with corresponding *p*-values <0.05), we used the expression from the probe set indicating the highest MAS5 expression intensity, which yielded expression-ratio estimates between replicates consistent with RNA-seq and qPCR, as detailed further in Results section. In general, log 2 Mas5 intensities >5 correspond to "present" calls (see Figure 6 and accompanying text on the dynamic range for further details). Affymetrix data are available at NCBI GEO, at the accession number GSE124945.

Data Mining. TCGA data for ovarian cancer (OV) and lung squamous cell carcinoma (LUSC) assayed by RNA-seq were downloaded from xena.ucsc.edu, as estimated gene counts and TPMs for each gene in each TCGA sample, analyzed via the TOIL pipeline.[11] TCGA data for OV and LUSC, assayed by Affymetrix HG U133a arrays, were obtained from GEO (accession numbers GSE68661 and GSE68793 for OV and LUSC, respectively) and were analyzed in R, using the methods described above for Affymetrix arrays. For the computation of expression ratios between samples, estimated counts from the TOIL pipeline were input into edgeR, to obtain normalized gene expression in CPMs, allowing for the

DOI: 10.1021/acsomega.9b02811
ACS Omega 2019, 4, 17048−17059

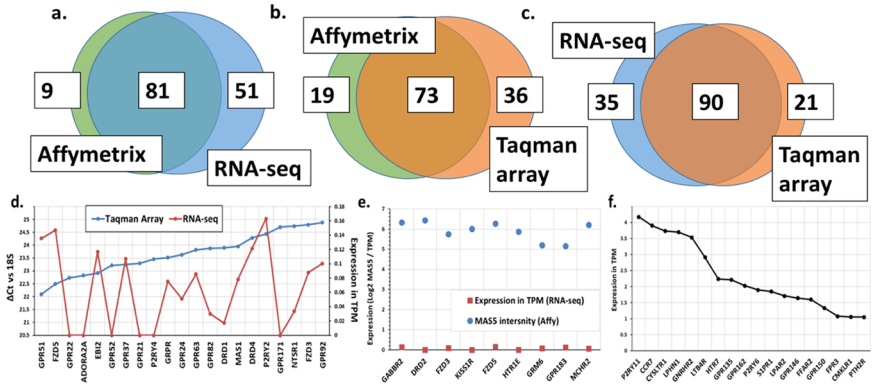

Figure 1. Detection of GPCRs by RNA-seq, TaqMan GPCR arrays, and Affymetrix (Affy) arrays. (a–c) GPCRs for which the relevant primer probes are present by each method. Representative data are shown for an individual CAF replicate as an example; similar numbers were detected by all three methods in a second replicate. (d) Differences in GPCR expression between RNA-seq and TaqMan arrays. (e) False-positive detection of GPCRs from Affymetrix HG U133plus2.0 arrays; these GPCRs were detected by neither RNA-seq (plotted above) nor TaqMan arrays (not shown). (f) False negatives from Affymetrix arrays that we detected by the other methods; expression is plotted for such GPCRs identified by RNA-seq.

comparison of expression ratios for genes between pairs of samples. RNA-seq data from the CCLE[2] for cell lines were downloaded as gene expression in TPMs from the EBI expression atlas,[12] from data provided on that portal, analyzed via the iRAP pipeline.[13]

Cellular Calcium Assays. Intracellular calcium concentration of AsPC-1 cells was measured using the FLIPR-4 calcium assay reagent (Cat # R8142, Molecular Devices, San Jose, CA). In brief, cells were plated in black-walled clear-bottom 96-well plates overnight at ∼80% confluency using media and conditions described in Methods. Culture media was then removed and cells were incubated for 1 h at 37 °C, 5% CO_2 in FLIPR-4 loading buffer, consisting of FLIPR-4 reagent diluted (as per the manufacturer's instructions) in Hank's balanced salt solution (HBSS) (with calcium and magnesium) buffered with 20 mM *N*-(2-hydroxyethyl)-piperazine-*N*′-ethanesulfonic acid and 0.2% bovine serum albumin, with pH adjusted to 7.4. Loading buffer also contained probenecid (2.50 mM, Sigma-Aldrich, Cat # P8761) to prevent leakage of the calcium reagent from the cells. Calcium response was then measured via a FlexStation 3 Multi-Mode Microplate Reader (Molecular Devices). GPCR agonists were added, and response in relative fluorescence units was measured over 105 s for each well, yielding data for peak response and kinetics of response. For calcium assays and wound-healing assays, we used the following GPCR agonists: Neurotensin (Cat # 1909, Tocris, Minneapolis, MN); 2-Thio-UTP (Cat # 3280, Tocris); histamine (Cat # AAJ6172703, Fischer Scientific); oxytocin (Cat # 1910, Tocris); and sulprostone (Cat # 14765, Cayman Chemical).

Migration/Wound-Healing Assays. Rate of migration of AsPC-1 cells was estimated using a scratch-wound assay. Cells were plated in 24-well plates and grown to approximate confluency. A scratch was made in each well using a 200 μL pipette tip, culture media was replaced to remove floating cells, and the scratches were imaged using a BZ-X700 microscope. Cells were then incubated with GPCR agonists at concentrations described in the following sections and were returned to a 37 °C, 5% CO_2 incubator. After 24 h, the same scratches were imaged once again. The area of scratches at the 0 and 24 h time points was then calculated via standard protocols in ImageJ v1.52a to evaluate wound closure. Migration data were analyzed for statistical significance using the Prism Graphpad (GraphPad Software, San Diego, CA) via one-way analysis of variance (ANOVA) with Tukey multiple comparison testing.

RESULTS

Comparison of GPCR Expression Data for Pancreatic CAFs. Table S2 (top) shows the number of GPCRs each method can detect, based on limitations of the number of primers (TaqMan arrays) or probes (Affymetrix arrays). Both methods should allow the detection of a similar number of endoGPCRs. TaqMan arrays are not designed to detect chemosensory GPCRs, and Affymetrix arrays also have relatively few probe sets for chemosensory GPCRs. Figure 1 and Table S2 (bottom) show that the number of endoGPCRs in pancreatic CAFs detected by RNA-seq and TaqMan arrays is greater than is detected by Affymetrix arrays. The threshold of detection used for determining whether a GPCR was detected in RNA-seq data was set to 0.2 TPM, based on the analysis discussed in Figure S1 and accompanying text. Detection thresholds for TaqMan arrays and Affymetrix arrays are discussed in Methods section.

RNA-seq identified the greatest number of GPCRs, likely because this method is not limited by a fixed number of probes/primers. RNA-seq and Affymetrix HG U133plus2.0 arrays both detect a small number of chemosensory GPCRs; their level of expression was typically just above the detection thresholds defined above and in Methods section. Both RNA-seq and TaqMan arrays identified in common most of the detected GPCRs. Virtually all highly expressed GPCR identified by either TaqMan arrays or RNA-seq were commonly detected by both, whereas Affymetrix arrays detected fewer GPCRs in common (Figure 1a–c). GPCRs uniquely identified by each method were typically expressed at very low levels, i.e., near detection thresholds. Eight endoGPCRs were detected by RNA-seq but not by TaqMan arrays due to the absence of corresponding primers on the TaqMan arrays.

The overall agreement between TaqMan arrays and RNA-seq is further illustrated in Figure 1d–f: the 21 GPCRs detected by TaqMan arrays but that were below thresholds for the detection by RNA-seq were all expressed at >22 cycles above 18 S (i.e., >∼33 qPCR cycles), implying low expression levels of these receptors by either method (Figure 1d). Thus,

DOI: 10.1021/acsomega.9b02811
ACS Omega 2019, 4, 17048−17059

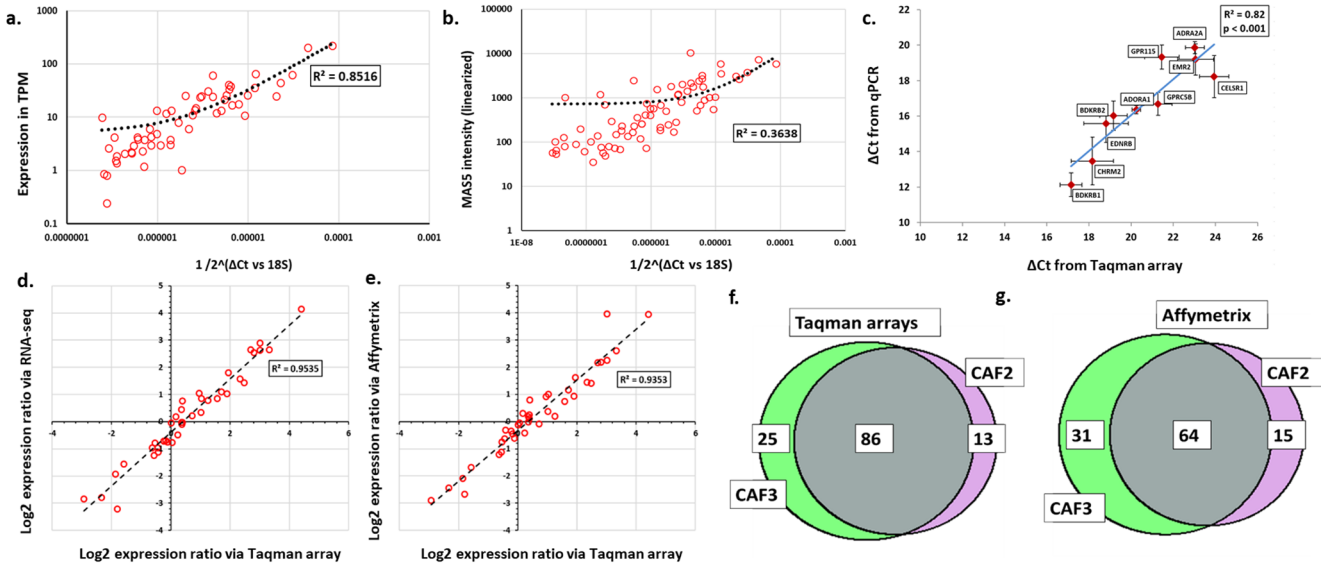

Figure 2. Comparison of GPCR expression levels by RNA-seq, TaqMan GPCR arrays, and Affymetrix (Affy) arrays with independent qPCR and comparisons of expression changes. (a) Data from RNA-seq compared to that of TaqMan arrays; (b) data from Affymetrix HG U133plus2.0 arrays compared to that of TaqMan arrays. Representative data are shown for an individual CAF sample. (c) Validation of TaqMan GPCR array data by qPCR, for $N = 5$ CAF samples; the data shown are mean and standard error of the mean (SEM) of ΔCt vs 18 S rRNA. (d, e) Correlation between expression ratios of GPCRs in two CAF samples (CAF2 and CAF3) evaluated by (d) RNA-seq and TaqMan arrays and (e) Affymetrix HG U133plus2.0 and TaqMan arrays. (f, g) Number of GPCRs in two CAF samples as detected by (f) TaqMan arrays and (g) Affymetrix HG U133plus2.0 arrays.

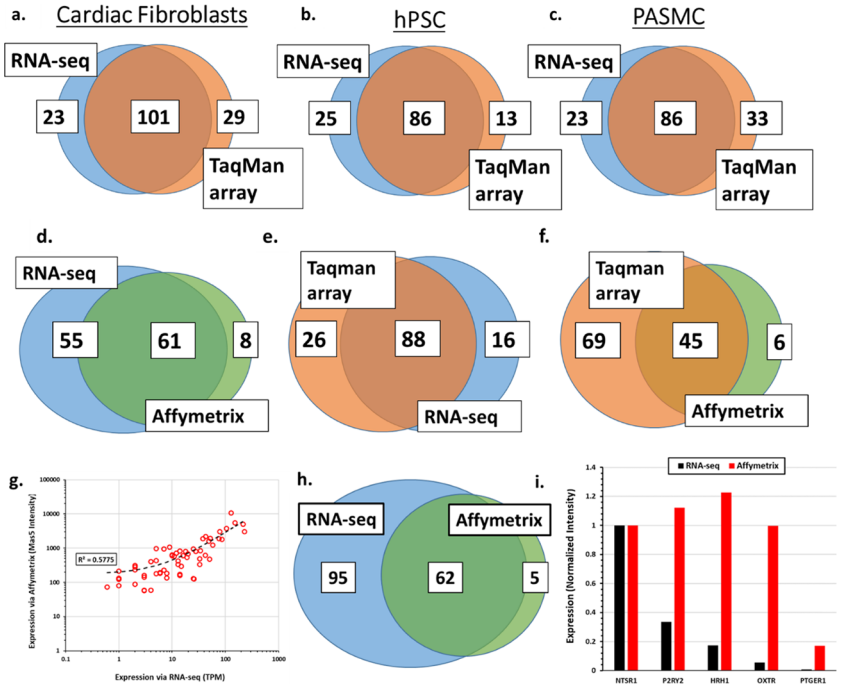

Figure 3. GPCR expression in other cell types. (a–c) Number of GPCRs detectable by RNA-seq and TaqMan arrays in individual human lines of (a) primary fetal cardiac fibroblasts, (b) PSCs, and (c) PASMCs. (d–f) The number of GPCRs expressed by the AsPC-1 pancreatic ductal adenocarcinoma cell line (determined by Affymetrix HG U133plus2.0 arrays; CCLE), TaqMan GPCR arrays (Insel Lab), and RNA-seq (CCLE and EBI). (g, h) GPCR expression of MDA-MB-231 breast cancer cells (determined by Affymetrix HG U133plus2.0 arrays and RNA-seq; CCLE). (g) Correlation in the GPCR detection by the two methods for the 62 commonly detected GPCRs. (h) The number of commonly or uniquely identified GPCRs using RNA-seq or Affymetrix HG U133plus2.0 arrays. (i) For CCLE data, expression in AsPC-1 cells of five Gq-coupled GPCRs tested for functional effects in Figure 7, linearized (for Mas5 data) and normalized to the expression of NTSR1, the highest expressed of these receptors as per RNA-seq data.

all highly expressed GPCRs identified by TaqMan arrays are also detected by RNA-seq. We found a small number of apparent false positives from Affymetrix data, i.e., GPCRs not detectable by either TaqMan arrays or RNA-seq (Figure 1e)

DOI: 10.1021/acsomega.9b02811
ACS Omega 2019, 4, 17048−17059

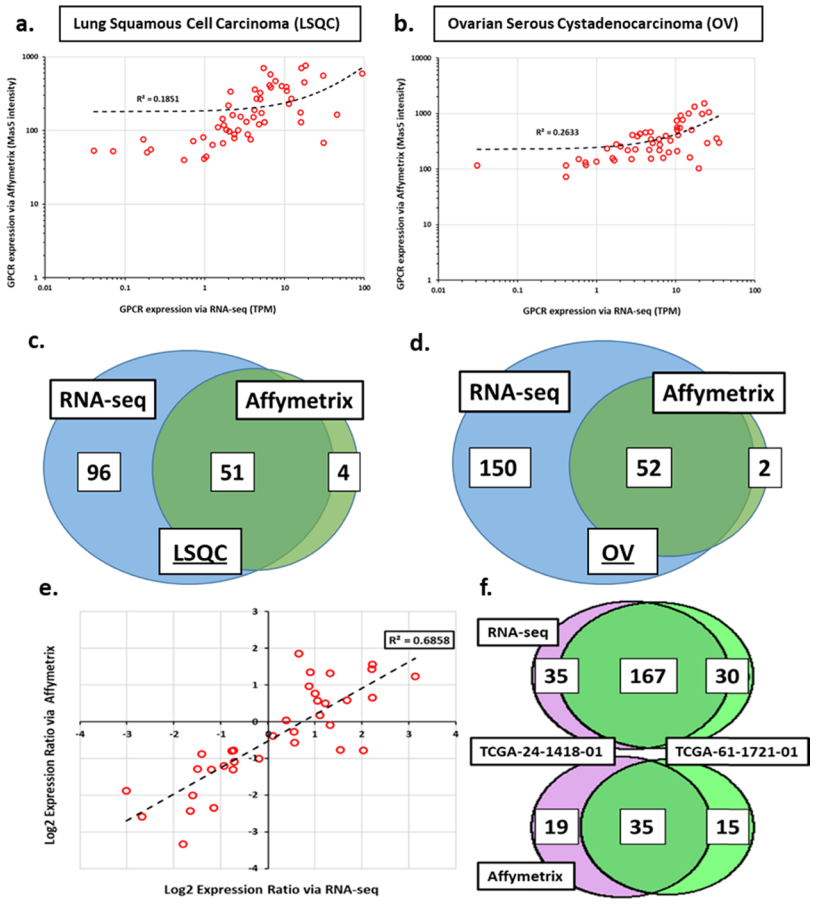

Figure 4. Comparison of GPCR expression data in TCGA samples generated by Affymetrix arrays and RNA-seq. (a, b) The correlation of expression of commonly detected GPCRs and (c, d) Venn diagrams showing the overlap in GPCR expression of randomly selected tumor samples assessed by Affymetrix HG U133a arrays or RNA-seq of ovarian cancer (OV; TCGA24-1418-01) and LUSC (TCGA-37-4141-01) tumor samples in TCGA. (e) The correlation of expression ratios and (f) Venn diagrams of GPCRs detected by RNA-seq or Affymetrix HG U133a array for a randomly selected pair of TCGA OV samples.

and numerous false negatives from Affymetrix data (GPCRs detected by RNA-seq and/or TaqMan arrays) (Figure 1f). The apparent false positives in the Affymetrix data were relatively low-expressed (Log 2 MAS5 intensity <7). TaqMan arrays and RNA-seq show a relatively high correlation (R^2 > 0.8) in the magnitude of GPCR expression (Figure 2a) but data from Affymetrix arrays correlate poorly (R^2 < 0.4) with results from TaqMan arrays (Figure 2b) and RNA-seq (shown for various cells/tissues in subsequent sections).

Independent qPCR using SYBR green and primers designed in our lab was used to validate GPCR expression measured by the three methods. Figure 2c shows the average expression of 10 GPCRs in CAFs derived from five different patients, assayed via independent qPCR and the correspondence of these data with TaqMan array data. We found a high degree of correspondence with results from TaqMan arrays and qPCR (R^2 ∼ 0.8) and between results from RNA-seq and qPCR (R^2 ∼ 0.8, not plotted) but not from Affymetrix arrays and qPCR (R^2 < 0.5, not plotted).

Although Affymetrix HG U133plus2.0 arrays did not provide gene abundance estimates comparable with either RNA-seq or qPCR-based arrays, if one estimates expression ratios among biological replicates (an indication of how much a gene's expression differs among samples), results for all three methods are in close agreement. Figure 2d,e shows this for ∼40 GPCRs commonly detected in two CAF samples by all three methods: expression differences among samples are nearly equal for the three methods.

Are these methods equally useful for evaluating changes in expression between samples? Figure 2f,g shows the overlap of detected GPCRs for two biological replicates (CAF2 and CAF3) assessed by TaqMan arrays (RNA-seq performs nearly identically[3]) and Affymetrix HG U133plus2.0 arrays. A smaller proportion of detected GPCRs was observed for *n* replicates tested by the Affymetrix arrays. Fewer GPCRs are consistently detectable by Affymetrix HG U133plus2.0 arrays; the estimation of changes in GPCR expression is, thus, less feasible than with the other methods. However, for GPCRs that one can consistently quantify by Affymetrix arrays, estimates of differences in their expression are consistent with those of the other two methods. Figure 6 (and accompanying text) shows quantitative analysis for the dynamic range of detection of GPCRs by each method, from data in CAFs. Affymetrix arrays have a narrower dynamic range than TaqMan arrays or RNA-seq, which both show very similar behavior. In addition, the correlation for all genes, in general, between RNA-seq and Affymetrix arrays appears poor.

Comparison of GPCR Expression Estimates in Other Cell Types. We obtained a similarly high degree of correspondence between TaqMan array and RNA-seq data in other cell types. Figure 3a−c shows the detection of GPCRs by TaqMan arrays and RNA-seq in human cardiac fibroblasts,

DOI: 10.1021/acsomega.9b02811
ACS Omega 2019, 4, 17048−17059

pancreatic stellate cells (PSCs), and pulmonary arterial smooth muscle cells (PASMCs). Most GPCRs are identified by these two methods in all three cell types. Similar to the data from CAFs, the GPCRs commonly detected by both TaqMan arrays and RNA-seq include all highly expressed GPCRs (e.g., those expressed >10 TPM). Thus, GPCR expression analysis by TaqMan arrays and RNA-seq is consistent in a variety of primary cell types.

To further test Affymetrix arrays with the two other methods, we assessed the expression of GPCRs in AsPC-1 PDAC cells using TaqMan arrays and compared these data with RNA-seq and Affymetrix HG U133plus2.0 array data for the same GPCRs from data in CCLE.[2] We found that our TaqMan array data and the CCLE RNA-seq data showed much better correspondence than did the CCLE Affymetrix data to either of those methods/sources (Figure 3d−f). Thus, GPCR expression determined by RNA-seq and TaqMan arrays assayed at different laboratories, batches of cell lines, media, etc. shows greater concordance than GPCR data from RNA-seq and Affymetrix arrays, for samples prepared in the same laboratory.

We also assessed data for another cell line (MDA-MB-231 breast cancer cells) from CCLE and the tumor tissue from TCGA. We compared data from CCLE using Affymetrix HG U133plus2.0 arrays and found a similarly poor correlation between GPCR expression assayed by the Affymetrix arrays compared to RNA-seq (Figure 3d,e). Fewer GPCRs were detected by the Affymetrix arrays than by RNA-seq, and the magnitudes of GPCR expression were poorly correlated (R^2 = 0.58). Figure 3i shows the expression in AsPC-1 cells (from CCLE data) of 5 Gq/11-coupled GPCRs determined by RNA-seq and Affymetrix arrays; these GPCRs were, subsequently, studied for their functional effects (Figure 7). RNA-seq reveals a range of expression levels between these GPCRs, with NTSR1 and P2RY2 very highly expressed, while the other highlighted receptors had lower expression. By contrast, data from Affymetrix arrays implied a similar, very high level of expression for four of these GPCRs. Consistent with the RNA-seq data, data from TaqMan arrays also showed that NTSR1 and P2RY2 are especially highly expressed in AsPC-1 pancreatic cancer cells (not shown), while the other receptors had lower expression.

Comparison of GPCR Expression Estimates in the Tumor Tissue. We next tested how well RNA-seq and the Affymetrix arrays compare in the assessment of GPCR expression in human tissues and in the ratios of GPCR expression in pairs of samples. For this comparison, we used gene expression data from The Cancer Genome Atlas (TCGA) for lung squamous cell carcinoma (LUSC) and ovarian cancer (OV) tumors. As we observed for cells, the two methods compare poorly in terms of number of GPCRs detected and magnitude of expression of individual GPCRs in the tissue samples. Figure 4a−d shows the relationship between RNA-seq and Affymetrix HG U133a array data from the same tumor/donors for representative LUSC and OV samples with poor correspondence for data by the two methods (R^2 = 0.19 for LUSC and R^2 = 0.26 for OV). RNA-seq identified many more GPCRs, but even for GPCRs detected by both methods, there was a poor correlation in the magnitudes of expression between the methods. The HG U133a arrays are an older, less comprehensive (i.e., a smaller number of probes) product than the HG U133plus2.0 arrays we tested with CAF samples, but large amounts of archived gene expression data use these or older arrays. Such archived data should, thus, likely be avoided for evaluating GPCR expression.

The assessment of GPCR expression between random pairs of tumor sample replicates reveals relatively poor ability to detect GPCR expression by Affymetrix HG U133a arrays compared to RNA-seq (Figure 4e,f). The ratios of expression also do not correlate between the two methods, thus providing further evidence that data from older generations of Affymetrix arrays are unlikely to yield accurate data regarding GPCR expression.

Evidence for GPCR "False Negatives" in TCGA Tumor Affymetrix Data. As noted in the examples shown for ovarian serous carcinoma (OV) and lung squamous cell carcinoma (LUSC) in TCGA data (Figure 4), numerous GPCRs are detected in tumors by RNA-seq but not Affymetrix arrays. Data in the literature document a functional role for many of these GPCRs, thus supporting the idea that these failures to detect GPCRs in Affymetrix data constitute false-negative results. Examples of such GPCRs in OV include the smoothened homologue receptor (SMO), which drives hedgehog signaling.[14] SMO has been implicated as a potential therapeutic target in ovarian cancer with substantial data implying a functional role for SMO.[15−17] However, Affymetrix arrays yield poor evidence for the detection of this gene, whereas RNA-seq reveals substantial expression. CXCR3,[18,19] CXCR6,[19,20] CXCR5,[19,21] and S1PR2[22] are additional examples of GPCRs with demonstrated functional effects in OV tumors that are detected by RNA-seq data but not by Affymetrix microarrays. Similarly, in LUSC, SMO, CXCR6, CXCR3, and CXCR5 are false negatives from Affymetrix data but are detected by RNA-seq and are functional GPCRs[23−27] in LUSC.

RNA-Seq Data Suggest That Splice Variation Occurs among GPCRs. An additional advantage of the use of RNA-seq to assess GPCR expression is its ability to identify alternatively spliced transcripts, a largely unexplored aspect for GPCRs. Approximately, 45−50% of GPCRs are intron-less, which may explain why splice variation in GPCRs has not been studied in detail.[28,29] We found that many GPCRs, in particular adhesion GPCRs, which have a large number of exons, may undergo alternate splicing. Figure 5a shows the number of GPCRs and those that express multiple splice

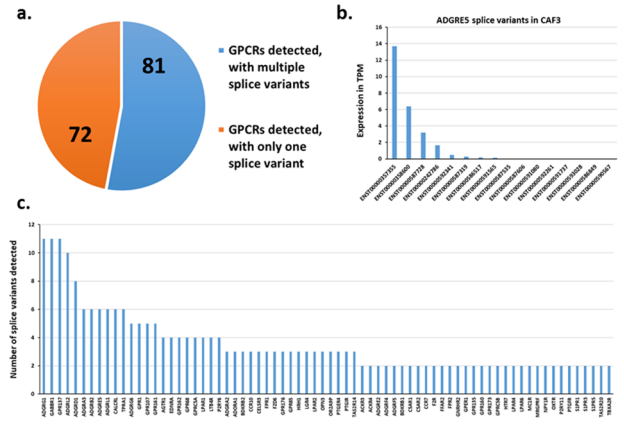

Figure 5. Expression of splice variants of GPCRs in CAFs: CAF3 as an example. (a) The number of GPCRs detected with multiple transcripts expressed at >0.2 TPM expression threshold. (b) As an example, the expression of different transcripts for ADGRE5 (aka CD97). (c) GPCRs with multiple transcripts detected and the number of transcripts expressed at >0.2 TPM for each GPCR.

DOI: 10.1021/acsomega.9b02811
ACS Omega 2019, 4, 17048−17059

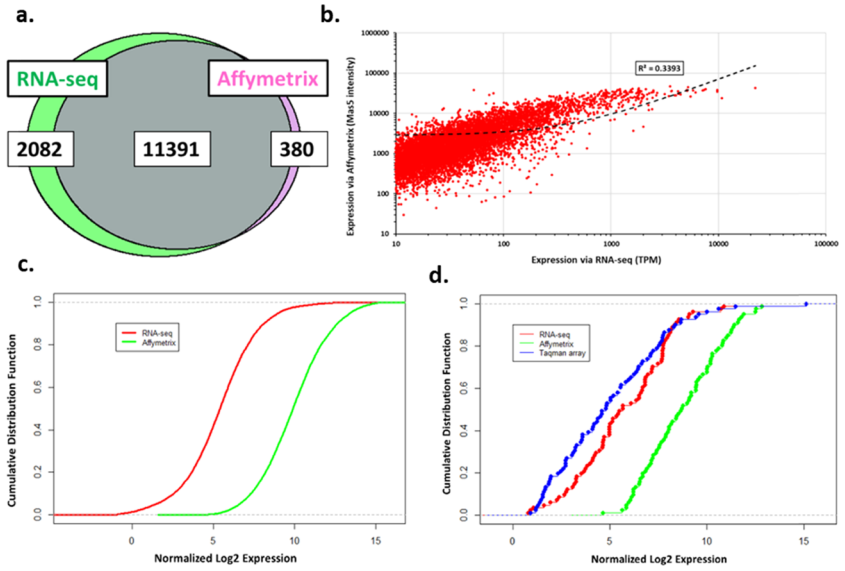

Figure 6. Gene expression and the dynamic range of detection by different methods. (a) Venn diagram of the detection of all protein-coding genes by Affymetrix HG U133plus2.0 arrays and RNA-seq in pancreatic CAFs. (b) Correlation of expression values for commonly detected genes by both the methods. (c, d) Cumulative distribution functions (CFDs) showing (c) the dynamic range of RNA-seq and Affymetrix arrays (HG U133plus2.0) for all genes; (d) the same as (c), but for GPCRs, detected by RNA-seq, Affymetrix arrays, and TaqMan arrays.

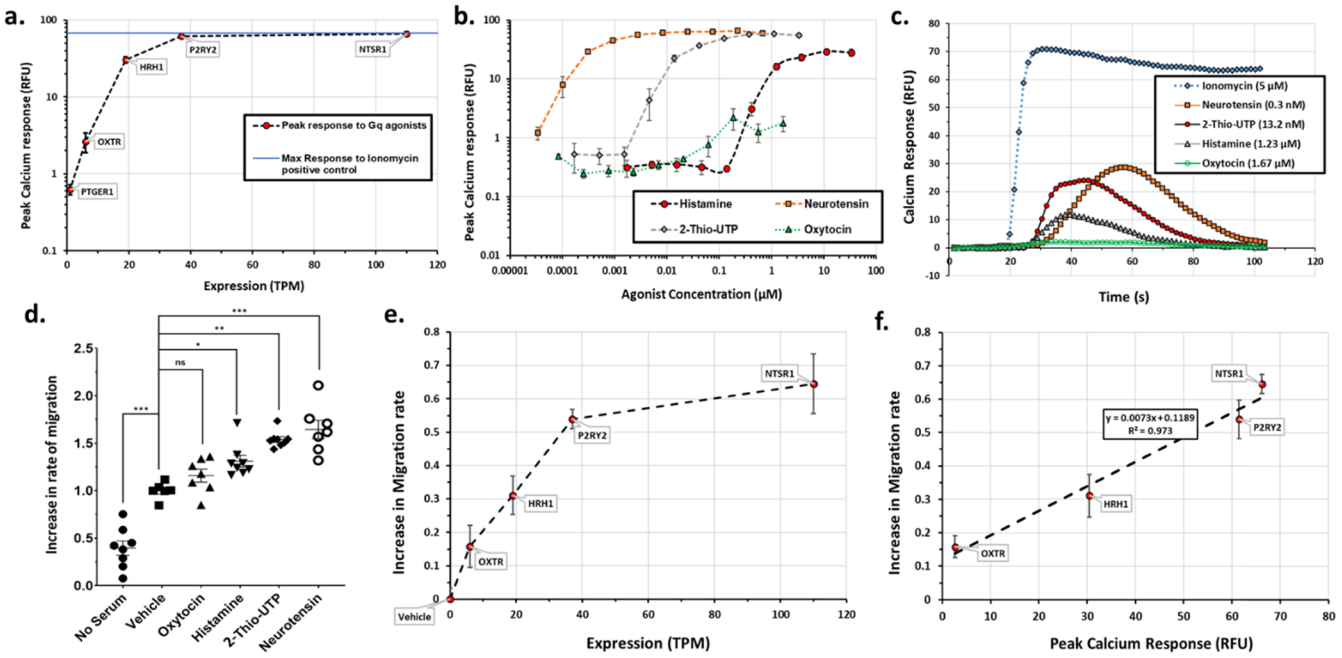

Figure 7. Signaling and functional response to agonists for Gq-coupled GPCRs in AsPC-1 cells. (a) Maximal GPCR agonist-promoted increase in intracellular calcium ["calcium response", relative to 5 μM ionomycin-induced response (blue line)] for agonists of the indicated GPCRs that are expressed at different TPM in AsPC-1 cells (as determined by RNA-seq in CCLE[2]). Data shown are the mean and SEM from three independent experiments. (b) Concentration−response curves for peak calcium response by the indicated GPCR agonists compared to GPCR expression as in panel (a). Data shown are mean and SEM, from three independent experiments. (c) Kinetics of calcium response by agonist concentrations that yield half-maximal response and kinetics of the ionomycin positive control; data shown are representative from individual wells in a 96-well plate; other replicates showed similar behavior. (d) Impact of treatment with GPCR agonists on the migration of AsPC-1 cells over 24 h; $N \geq 6$ for each treatment. Agonist concentrations were: oxytocin (5 μM); histamine (10 μM); 2-Thio-UTP (0.5 μM), neurotensin (0.1 μM); *: $p < 0.05$; **: $p < 0.001$; ***: $p < 0.0001$; significance was evaluated via one-way ANOVA with Tukey multiple comparison testing. (e) The relationship between the increased rate of migration and GPCR expression [as in panel (a)]. (f) The relationship between maximal calcium response promoted by the GPCR agonist concentrations indicated in (d) and the increase in the rate of migration of AsPC-1 cells.

variants in a human pancreatic CAF sample. Nearly, half of all identified GPCRs appears to show alternative splicing. As an example, ADGRE5/CD97, an adhesion GPCR, appears to have at least five meaningfully expressed splice variants (Figure 5b). These data were obtained at moderate sequencing depth; to more precisely identify the presence of particular splice variants in individual samples and cell types, one requires a greater sequencing depth (e.g., sequencing with 150 base-pair,

DOI: 10.1021/acsomega.9b02811
ACS Omega 2019, 4, 17048−17059

paired-end reads). Subsequent studies would then be needed to define the biological activity of such variants. Of the three methods used here, only RNA-seq can define alternative splicing of GPCRs and with bioinformatics tools (such as Kallisto[4]) can quantify transcript levels. Figure 5c shows the number of detected variants for each GPCR where we noted evidence for splice variation.

Comparison of the Dynamic Range between Methods. To determine how the detection of GPCRs compares with that of the expression of all protein-coding genes, we compared the dynamic range of detection for those genes by Affymetrix HG U133plus2.0 arrays and RNA-seq. For estimating the dynamic range of detection for GPCRs, we also included TaqMan GPCR arrays. We found (Figure 6a) that RNA-seq detects more genes but RNA-seq and Affymetrix arrays largely detect the expression of the same genes. The latter finding contrasts with the results for GPCRs and likely results from the relatively low expression of some GPCRs and the limited ability of Affymetrix arrays to detect low abundance transcripts. For most other genes/mRNAs, especially those with intermediate or high expression, the two methods perform similarly, although the magnitude of expression of commonly detected genes does not correlate well between the two methods (Figure 6b).

Figure 6c shows the dynamic range of detection for all transcripts by RNA-seq and Affymetrix arrays; gene expression was normalized to log 2 units (i.e., log 2 of TPM expression for RNA-seq and MAS5 intensity for Affymetrix arrays). We added a small constant to RNA-seq expression values, so that the log 2 of the highest expression value in TPM = log 2 of the highest expression value in MAS5 intensity. To evaluate the dynamic range for detection by each method, we computed the cumulative distribution function (CDF) for each set of expression values. RNA-seq had a larger detection range (~50-fold) and could detect genes ranging from ~15 to ~0 adjusted log 2 TPM, whereas Mas5 log 2 intensities ranged from ~15 to ~5. Figure 6d shows a similar trend for GPCRs with respect to the dynamic range for RNA-seq, TaqMan arrays, and Affymetrix arrays. GPCR expression was normalized as log 2 units (as above) with a small normalization factor added to TaqMan array data and RNA-seq data, so that log 2 expression of GAPDH (in all three datasets as a housekeeping gene) was equal and served as the first point (from the right) on the CDF. As the highest expressed gene that was commonly detectable across all three platforms, GAPDH was used as the housekeeping gene for this comparison. The range of expression levels between GAPDH and the lowest-detectable level of GPCR expression allows us to define and compare the dynamic range for each assay. TaqMan arrays and RNA-seq had a similar dynamic range, consistent with the high degree of correlation between the two methods; the dynamic range was lower with Affymetrix arrays.

GPCR mRNA Expression Shows Concordance with Signaling and Functional Response. To validate the GPCR expression data, we tested whether the level of mRNA expression can predict GPCR response with respect to signaling and functional activities. We opted to study a set of GPCRs which couple to Gq/11 Gα proteins, thus signaling via increases in intracellular calcium: the neurotensin receptor (NTSR1), the P2Y2 purinergic GPCR (P2RY2), the histamine H1 receptor (HRH1), the oxytocin receptor (OXTR), and the EP1 prostaglandin receptor (PTGER1), spanning a range of expression (assayed via RNA-seq in CCLE[2]) from >100 TPM (NTSR1) to 1 TPM (PTGER1) in AsPC-1 pancreatic cancer cells (Figure 7a). All five GPCRs have well-known agonists that act via Gq/11:[14] neurotensin (NTSR1), 2-Thio-UTP (P2RY2), histamine (HRH1), oxytocin (OXTR), and sulprostone (PTGER1). Each agonist should activate the specified receptor due to their known pharmacology and based on the GPCRs expressed in AsPC-1 cells. For example, HRH1 is the only HRH receptor, OXTR is the only vasopressin and oxytocin receptor family member expressed and among targets for sulprostone, PTGER1 is the only one expressed in AsPC-1 cells. Similarly, P2RY2 is the only purinergic GPCR expressed, which is activated by 2-Thio-UTP.

We first tested the calcium response (i.e., the increase in cytosolic calcium) in AsPC-1 cells for each agonist, over a range of concentrations. Figure 7a shows the peak ("maximal") calcium signal recorded for each ligand [at saturating concentrations (Figure 7b)] as a function of the magnitude of expression of its cognate GPCR target. We observed a sigmoidal behavior, wherein the calcium response plateaus for highly expressed GPCRs; the maximal signal was equal to that elicited by ionomycin, a positive control. PTGER1 did not elicit a signal, implying that one TPM may be a threshold for the detection of Gq/11 signaling in these cells by this method. Figure 7b shows the concentration−response for each agonist that increases the cytosolic calcium. The apparent EC_{50} values for these ligands vary somewhat from values in the literature, e.g., the EC_{50} for neurotensin signaling at NTSR1 is ~0.3 nM, approximately an order of magnitude lower than that reported in the literature.[14] This raises the possibility that signaling in native cells may differ from that in model systems where such data are typically generated. The kinetics for ionomycin and for agonists at concentrations approximately corresponding to half-maximal response (Figure 7c) suggest differences in the rates of activation of the different GPCRs, although the calcium transient is ~60−90 s in all cases.

We next tested the ability of these agonists (excluding sulprostone, as we obtained no evidence of calcium response for this compound), to stimulate migration (using a wound-healing assay) at concentrations that correspond to maximal activation of their respective GPCRs. Figure 7d shows the effect of agonist treatment on the rate of wound closure, compared with vehicle-treated cells. We used cells plated without the serum as a negative control. Higher GPCR expression and stronger calcium response result in greater stimulation of migration (Figure 7e,f), thus allowing us to relate GPCR expression, signaling, and functional response. Based on data in Figure 3i, Affymetrix data in the same cell line, from the same source (CCLE) failed to resolve the differences in expression between these GPCRs that were observed via RNA-seq. As a consequence, the data from the Affymetrix arrays did not permit accurate identification and stratification of GPCRs based on their expression and hence those results could not reliably predict which GPCRs were highly enough expressed to yield a strong functional response. Thus, data from Affymetrix arrays do not reliably identify the GPCRs that are most highly expressed. In screening for expression of GPCRs for subsequent drug/target discovery studies, Affymetrix arrays should likely be avoided in favor of other methods.

DISCUSSION

The comparison of three methods for high-content screening of GPCR mRNA expression reveals that TaqMan GPCR arrays

DOI: 10.1021/acsomega.9b02811
ACS Omega 2019, 4, 17048−17059

and RNA-seq show comparable performance, whereas Affymetrix arrays perform at a lower level. A likely reason for the latter result is the generally low expression of GPCRs, such that they are outside the dynamic range for optimal detection by arrays designed to assess the entire transcriptome. Highly expressed GPCRs, especially ones that are well characterized, are generally reliably detected by either TaqMan GPCR arrays or RNA-seq. By contrast, Affymetrix arrays fail to identify large numbers of GPCRs and show the poor correlation of expression and estimates for changes in expression compared to the other two methods. GPCRs, as a large family of genes, with a large (3 orders of magnitude) range of expression provide additional support for the accuracy and completeness, especially of RNA-seq data, and complement other validation studies.[30] The numerous false negatives observed with Affymetrix data are likely attributable to lower sensitivity, i.e., for expression thresholds <4−5 TPM in corresponding RNA-seq data, GPCRs will frequently be undetected by Affymetrix arrays.

The comparison of the three methods (Table 1) shows that TaqMan arrays or RNA-seq are preferable for GPCR detection and profiling. TaqMan arrays require minimal bioinformatic effort and, thus, can rapidly generate data. Important advantages of RNA-seq include: (1) the number of GPCRs that are potentially detectable (Table S2), since gene-specific primers or probes are not needed and (2) RNA-seq detects non-GPCR genes (including data for post-GPCR signaling components), yielding far more information than do TaqMan arrays. RNA-seq, thus, has the potential to explore other aspects of GPCR biology, such as pathways for cellular regulation.

As a consequence of the ongoing decrease in the cost of sequencing, the potentially lower expense to conduct RNA-seq is another advantage of this technique. A "hidden" cost of RNA-seq involves data analysis and storage, which can substantially increase the expenditure for RNA-seq. RNA-seq requires time for library preparation and sequencing as well as bioinformatic analysis. By contrast, data analysis of qPCR-based arrays can be done quickly. Other qPCR-based arrays are available that may yield comparable data but at a lower cost than TaqMan arrays, e.g., SYBR green-based arrays [e.g., Cat # 10034500 (Bio-Rad) and Cat # PAHS-071Z (Qiagen)].

A further advantage of RNA-seq is that it has become a method of choice for many large databases and consortia (e.g., TCGA and GTEx[31]). The abundance of such publicly available RNA-seq data facilitates data mining and yields information for new studies, including with respect to GPCR signaling components and how GPCRs and such components may have altered expression profiles during physiologic perturbations and in disease states. Limited public data are available for GPCR arrays so mining of such data is less feasible.

Affymetrix array-derived data is found in sources such as Gene Expression Omnibus (GEO) and other databases and for many years has been used for data mining. The findings here suggest that for GPCRs, mining of Affymetrix array data is not advisable. Moreover, to the extent that GPCRs may be differentially expressed in cells or tissues, such as in disease,[3] the large number of false-negative results from Affymetrix arrays may impact on other analyses, such as in pathways and networks, in which GPCRs may be involved. The inferior dynamic range of Affymetrix arrays is likely not limited to GPCRs and may impact on the detection of other low-expressed, but functionally important, genes. Thus, caution is

Table 1. Comparison of Three High-Content Assays for Identifying and Quantifying GPCR Expression

	TaqMan GPCR arrays	RNA-seq (75 bp, single reads, ~25 × 10^6 reads/sample)	Affymetrix arrays (HG U133plus2.0)
ability to detect genes	most endoGPCRs but very few other GPCR types	all annotated GPCRs (~800) and other genes in the reference genome used	most endoGPCRs, but a relatively small proportion of chemosensory GPCRs
quality of gene expression quantification	high sensitivity with repeatable, robust results	high sensitivity with repeatable, robust results	poor sensitivity, large numbers of false negatives
assay cost[a]	~$400/sample	<$200/sample	~$450/sample
analysis requirements	RQ manager (Invitrogen)	Relatively complex multistep analysis pipeline using multiple tools	standard algorithms such as MAS5/RMA, implementable in R
recommended amount of input (total) RNA	~1000 ng	~200 ng	~1000 ng
other factors	normalization requires the use of housekeeping genes, expression quantified as ΔCt vs the housekeeping gene	normalization is independent of housekeeping genes, gene expression quantified in units such as CPM/TPM	normalization is independent of housekeeping genes, expression quantified via MAS5/RMA intensity
data mining for GPCR expression	not widely available, but where such data are provided should be usable	usable, with appropriate attention to data normalization and standardization	mining of archived data, especially for older Affymetrix arrays not advised for GPCR expression
overall assessment	recommended for the focused study of GPCRs, especially for time-sensitive data; easy data analysis	recommended for the study of GPCRs but requires access to bioinformatics tools, plus maybe time-lag in the generation of gene expression data	not recommended to assess GPCR expression

[a]Costs shown are with academic pricing, these are subject to variation, depending on access to core facilities as well as institution type.

DOI: 10.1021/acsomega.9b02811
ACS Omega 2019, 4, 17048−17059

advised in the use of Affymetrix arrays and mining of Affymetrix array data. Moreover, the evidence cited above for OV and LUSC tumors supports our conclusion that Affymetrix arrays yield numerous false negatives, i.e., GPCR mRNAs that are not detected but that are functionally relevant.

The study of the "GPCRome" and individual GPCRs identified by the methods compared here has the potential to yield important insights regarding the regulation of cells and tissues in health and disease. Moreover, GPCRs are targeted by ∼35% of FDA- and EMA-approved drugs[1] and represent the largest family of drug targets. Given their high druggability, identification of GPCRs in novel contexts can aid in drug discovery efforts.[32] The current results and other data show that cells express large numbers of (>100) GPCRs; these include GPCRs targeted by approved drugs, orphan receptors, and many GPCRs for which tool compounds (but not approved drugs) may exist. Multiple studies of "GPCRomics" combined with signaling and functional analyses have revealed novel roles for GPCRs in numerous cell types.[3,8,32−37] A growing number of studies have also begun to reveal the extent to which the presence of splice variants among GPCRs may impact their functional activity.[28,29] Consequences of such alternative splicing include the presence of receptor isoforms with altered ligand binding (primarily due to changes in the N-terminus), altered downstream signaling (including "decoy" receptors that bind ligands but have no functional activity), and potential effects on receptor trafficking, internalization, and localization within specific cellular domains. This remains a largely understudied aspect of GPCR biology. The presence of numerous GPCR splice variants at the mRNA level underscores the need for further investigation.

Because mRNA expression may not necessarily predict protein expression, we undertook functional studies of Gq-coupled GPCRs to test the concordance of mRNA expression with signaling/functional data. In general, for GPCRs, direct measurement of protein expression has been challenging, due to (a) difficulty in obtaining well-validated antibodies and (b) the low magnitude of expression of GPCRs. Thus, indirect methods to verify protein expression are needed. Here, we show that GPCR mRNA expression predicts signaling and functional response for multiple Gq/11-coupled GPCRs in a pancreatic cancer cell line. Highly expressed GPCRs (e.g., NTSR1 and P2RY2), which are among the 10 most highly expressed GPCRs overall in these cells, show very strong agonist-induced increases in intracellular calcium response and prominent functional response (migration), both of which appear to saturate at high levels of GPCR expression. We are not aware of prior such data for Gq/G11-coupled GPCRs, in particular in native cells.

Other results that imply a concordance between mRNA expression and functional response of prostanoid receptors in fibroblasts[37] and adrenoceptors in induced pluripotent stem cell-derived cardiomyocytes[8] support this observation in other GPCR systems. Thus, encouraging initial data (including those shown here) suggest that GPCR expression data can provide a useful first step in drug/target discovery efforts, with highly expressed GPCRs (or differentially expressed GPCRs in disease) likely to be the favored candidates for subsequent validation. Further studies are needed to determine the extent to which GPCR expression predicts the intensity of downstream signaling events, such as protein phosphorylation, transcriptional regulation, etc. Affymetrix arrays are not recommended for such efforts, as they do not adequately distinguish between high-expressed and low-expressed GPCRs and, in addition, fail to detect many GPCRs.

The analysis of the dynamic range of the detection of Affymetrix arrays (Figure 6) shows that the failure of these arrays to distinguish between expression of GPCRs was not explainable by "saturation" of these arrays, i.e., requiring dilution of samples to better place them on a standard curve for detection. The Affymetrix arrays were able to resolve large differences in expression between highly expressed genes (e.g., GAPDH) and lower expressed genes (e.g., many GPCRs) over a dynamic range (∼3 orders of magnitude) consistent with previous observations.[38] This result implies that the failure to adequately resolve differences in GPCR expression is likely attributable to (a) the flawed probe design for specific GPCR genes and (b) the lack of sensitivity of Affymetrix arrays to resolve small differences in expression between genes, especially lower expressed genes, to the level of quantitative precision obtainable by RNA-seq.

Omics data such as those presented in this study reveal the high expression of numerous orphan GPCRs in human disease, for which such validation studies are more challenging. Given the apparent concordance between the magnitude of expression and functional response of GPCRs, such data highlight specific highly expressed orphan GPCRs as priority candidates for further study and for attempts at deorphanization.

The data presented here highlight aspects of GPCR biology that merit further study. These include: (a) what is the functional impact of alternative splicing of GPCRs? (b) the high expression of many orphan GPCRs underscores the importance for further deorphanization efforts; the physiological role of much of the GPCRome remains unknown; (c) given the abundance of GPCRs expressed in different cell types, do GPCRs that are more widely/ubiquitously expressed than others have a functional significance? (d) which mechanisms regulate the expression of individual or groups of GPCRs in particular cell types? We anticipate that GPCRomic efforts, in combination with other techniques, will help address such issues, advance understanding of GPCR biology, and aid in efforts to develop novel therapeutics.

■ ASSOCIATED CONTENT

Supporting Information

The Supporting Information is available free of charge on the ACS Publications website at DOI: 10.1021/acsomega.9b02811.

Information about samples analyzed, primer sequences, and additional details regarding omics methods used (Tables S1−S3); setting a detection threshold for RNA-seq data (Figure S1) (PDF)

■ AUTHOR INFORMATION

Corresponding Author

*E-mail: pinsel@ucsd.edu.

ORCID

Krishna Sriram: 0000-0002-2385-3626

Author Contributions

K.S., S.Z.W., M.W.G., C.S., and J.M. performed experiments. R.P.F. and A.M.L. isolated/provided CAFs and cancer cells. K.S. and K.M. analyzed data. K.S. and P.A.I. designed the study and wrote the manuscript. A.M.L. and P.A.I. edited the manuscript. All authors approved the final version of the text.

DOI: 10.1021/acsomega.9b02811
ACS Omega 2019, 4, 17048−17059

Notes

The authors declare no competing financial interest.

■ ACKNOWLEDGMENTS

Studies in our laboratories related to this topic were supported by research and training grants from the National Institutes of Health (CA121938, HL007444, CA189477, AG053568) with additional research support from the Department of Defense (W81XWH-14-1-0372), Bristol Myers Squibb, an ASPET David Lehr Award and the Padres Pedal the Cause PTC2017 award. Data generated by the The Cancer Genome Atlas (TCGA) Research Network were used in this study.

■ ABBREVIATIONS

CPM, counts per million; TPM, transcripts per million; ΔCt, Δ/difference in cycle threshold; PDAC, Pancreatic Ductal Adenocacrinoma; FGF2, Fibroblast Growth Factor 2

■ REFERENCES

(1) Sriram, K.; Insel, P. A. G Protein-Coupled Receptors as Targets for Approved Drugs: How Many Targets and How Many Drugs? *Mol. Pharmacol.* **2018**, *93*, 251−258.

(2) Barretina, J.; Caponigro, G.; Stransky, N.; Venkatesan, K.; Margolin, A. A.; Kim, S.; Wilson, C. J.; Lehár, J.; Kryukov, G. V.; Sonkin, D.; et al. The Cancer Cell Line Encyclopedia Enables Predictive Modelling of Anticancer Drug Sensitivity. *Nature* **2012**, *483*, 603−607.

(3) Wiley, S. Z.; Sriram, K.; Liang, W.; Chang, S. E.; French, R.; McCann, T.; Sicklick, J.; Nishihara, H.; Lowy, A. M.; Insel, P. A. GPR68, a Proton-Sensing GPCR, Mediates Interaction of Cancer-Associated Fibroblasts and Cancer Cells. *FASEB J.* **2018**, *32*, 1170−1183.

(4) Bray, N. L.; Pimentel, H.; Melsted, P.; Pachter, L. Near-Optimal Probabilistic RNA-Seq Quantification. *Nat. Biotechnol.* **2016**, *34*, 525−527.

(5) Pimentel, H.; Bray, N. L.; Puente, S.; Melsted, P.; Pachter, L. Differential Analysis of RNA-Seq Incorporating Quantification Uncertainty. *Nat. Methods* **2017**, *14*, 687−690.

(6) Soneson, C.; Love, M. I.; Robinson, M. D. Differential Analyses for RNA-Seq: Transcript-Level Estimates Improve Gene-Level Inferences. *F1000Research* **2015**, *4*, 1521.

(7) Robinson, M. D.; McCarthy, D. J.; Smyth, G. K. EdgeR: A Bioconductor Package for Differential Expression Analysis of Digital Gene Expression Data. *Bioinformatics* **2010**, *26*, 139−140.

(8) Jung, G.; Fajardo, G.; Ribeiro, A. J. S.; Kooiker, K. B.; Coronado, M.; Zhao, M.; Hu, D.-Q.; Reddy, S.; Kodo, K.; Sriram, K.; et al. Time-Dependent Evolution of Functional vs. Remodeling Signaling in Induced Pluripotent Stem Cell-Derived Cardiomyocytes and Induced Maturation with Biomechanical Stimulation. *FASEB J.* **2016**, *30*, 1464−1479.

(9) Insel, P. A.; Sriram, K.; Wiley, S. Z.; Wilderman, A.; Katakia, T.; McCann, T.; Yokouchi, H.; Zhang, L.; Corriden, R.; Liu, D.; et al. GPCRomics: GPCR Expression in Cancer Cells and Tumors Identifies New, Potential Biomarkers and Therapeutic Targets. *Front. Pharmacol.* **2018**, No. 431.

(10) Gautier, L.; Cope, L.; Bolstad, B. M.; Irizarry, R. A. Affy–Analysis of Affymetrix GeneChip Data at the Probe Level. *Bioinformatics* **2004**, *20*, 307−315.

(11) Vivian, J.; Rao, A. A.; Nothaft, F. A.; Ketchum, C.; Armstrong, J.; Novak, A.; Pfeil, J.; Narkizian, J.; Deran, A. D.; Musselman-Brown, A.; et al. Toil Enables Reproducible, Open Source, Big Biomedical Data Analyses. *Nat. Biotechnol.* **2017**, *35*, 314−316.

(12) Kapushesky, M.; Emam, I.; Holloway, E.; Kurnosov, P.; Zorin, A.; Malone, J.; Rustici, G.; Williams, E.; Parkinson, H.; Brazma, A. Gene Expression Atlas at the European Bioinformatics Institute. *Nucleic Acids Res.* **2010**, *38*, D690−D698.

(13) Fonseca, N. A.; Petryszak, R.; Marioni, J.; Brazma, A. IRAP - an Integrated RNA-Seq Analysis Pipeline. *bioRxiv* **2014**, No. 005991.

(14) Alexander, S. P.; Christopoulos, A.; Davenport, A. P.; Kelly, E.; Marrion, N. V.; Peters, J. A.; Faccenda, E.; Harding, S. D.; Pawson, A. J.; Sharman, J. L.; Southan, C.; Davies, J. A.; CGTP Collaborators. The Concise Guide to Pharmacology 2017/18: G protein-coupled receptors. *Br. J. Pharmacol.* **2017**, *174*, S17−S129.

(15) Bhattacharya, R.; Kwon, J.; Ali, B.; Wang, E.; Patra, S.; Shridhar, V.; Mukherjee, P. Role of hedgehog signaling in ovarian cancer. *Clin. Cancer Res.* **2008**, *14*, 7659−7666.

(16) Steg, A. D.; Katre, A. A.; Bevis, K. S.; Ziebarth, A.; Dobbin, Z. C.; Shah, M. M.; Alvarez, R. D.; Landen, C. N. Smoothened antagonists reverse taxane resistance in ovarian cancer. *Mol. Cancer Ther.* **2012**, *11*, 1587−1597.

(17) McCann, C. K.; Growdon, W. B.; Kulkarni-Datar, K.; Curley, M. D.; Friel, A. M.; Proctor, J. L.; Sheikh, H.; Deyneko, I.; Ferguson, J. A.; Vathipadiekal, V.; Birrer, M. J.; et al. Inhibition of Hedgehog signaling antagonizes serous ovarian cancer growth in a primary xenograft model. *PloS One* **2011**, *6*, No. e28077.

(18) Lieber, S.; Reinartz, S.; Raifer, H.; Finkernagel, F.; Dreyer, T.; Bronger, H.; Jansen, J. M.; Wagner, U.; Worzfeld, T.; Müller, R.; Huber, M. Prognosis of ovarian cancer is associated with effector memory CD8+ T cell accumulation in ascites, CXCL9 levels and activation-triggered signal transduction in T cells. *Oncoimmunology* **2018**, *7*, No. e1424672.

(19) Rainczuk, A.; Rao, J.; Gathercole, J.; Stephens, A. N. The emerging role of CXC chemokines in epithelial ovarian cancer. *Reproduction* **2012**, *144*, 303.

(20) Mir, H.; Kaur, G.; Kapur, N.; Bae, S.; Lillard, J. W.; Singh, S. Higher CXCL16 exodomain is associated with aggressive ovarian cancer and promotes the disease by CXCR6 activation and MMP modulation. *Sci. Rep.* **2019**, *9*, No. 2527.

(21) Son, D. S.; Kabir, S. M.; Dong, Y.; Lee, E.; Adunyah, S. E. Characteristics of chemokine signatures elicited by EGF and TNF in ovarian cancer cells. *J. Inflammation* **2013**, *10*, No. 25.

(22) Beach, J. A.; Aspuria, P. J.; Cheon, D. J.; Lawrenson, K.; Agadjanian, H.; Walsh, C. S.; Karlan, B. Y.; Orsulic, S. Sphingosine kinase 1 is required for TGF-β mediated fibroblast-to-myofibroblast differentiation in ovarian cancer. *Oncotarget* **2016**, *7*, 4167.

(23) Abe, Y.; Tanaka, N. The hedgehog signaling networks in lung cancer: The mechanisms and roles in tumor progression and implications for cancer therapy. *BioMed Res. Int.* **2016**, No. 7969286.

(24) Huang, L.; Walter, V.; Hayes, D. N.; Onaitis, M. Hedgehog−GLI signaling inhibition suppresses tumor growth in squamous lung cancer. *Clin. Cancer Res.* **2014**, *20*, 1566−1575.

(25) Mir, H.; Singh, R.; Kloecker, G. H.; Lillard, J. W., Jr.; Singh, S. CXCR6 expression in non-small cell lung carcinoma supports metastatic process via modulating metalloproteinases. *Oncotarget* **2015**, *6*, 9985.

(26) Rivas-Fuentes, S.; Salgado-Aguayo, A.; Belloso, S. P.; Rosete, P. G.; Alvarado-Vásquez, N.; Aquino-Jarquin, G. Role of chemokines in non-small cell lung cancer: angiogenesis and inflammation. *J. Cancer* **2015**, *6*, 938.

(27) Singh, R.; Gupta, P.; Kloecker, G. H.; Singh, S.; Lillard, J. W., Jr. Expression and clinical significance of CXCR5/CXCL13 in human non-small cell lung carcinoma. *Int. J. Oncol.* **2014**, *45*, 2232−2240.

(28) Markovic, D.; Challiss, R. A. J. Alternative Splicing of G Protein-Coupled Receptors: Physiology and Pathophysiology. *Cell. Mol. Life Sci.* **2009**, *66*, 3337−3352.

(29) Oladosu, F. A.; Maixner, W.; Nackley, A. G. Alternative Splicing of G Protein-Coupled Receptors: Relevance to Pain Management. *Mayo Clin. Proc.* **2015**, *90*, 1135−1151.

(30) Wang, C.; Gong, B.; Bushel, P. R.; Thierry-Mieg, J.; Thierry-Mieg, D.; Xu, J.; Fang, H.; Hong, H.; Shen, J.; Su, Z.; et al. The Concordance between RNA-Seq and Microarray Data Depends on Chemical Treatment and Transcript Abundance. *Nat. Biotechnol.* **2014**, *32*, 926−932.

(31) GTEx Consortium. The Genotype-Tissue Expression (GTEx) Project. *Nat. Genet.* **2013**, *45*, 580−585.

DOI: 10.1021/acsomega.9b02811
ACS Omega 2019, 4, 17048−17059

(32) Insel, P. A.; Wilderman, A.; Zambon, A. C.; Snead, A. N.; Murray, F.; Aroonsakool, N.; McDonald, D. S.; Zhou, S.; McCann, T.; Zhang, L.; et al. G Protein-Coupled Receptor (GPCR) Expression in Native Cells: "Novel" EndoGPCRs as Physiologic Regulators and Therapeutic Targets. *Mol. Pharmacol.* **2015**, *88*, 181−187.
(33) Snead, A. N.; Insel, P. A. Defining the Cellular Repertoire of GPCRs Identifies a Profibrotic Role for the Most Highly Expressed Receptor, Protease-Activated Receptor 1, in Cardiac Fibroblasts. *FASEB J.* **2012**, *26*, 4540−4547.
(34) Amisten, S. Quantification of the MRNA Expression of G Protein-Coupled Receptors in Human Adipose Tissue. *Methods in Cell Biology*; Elsevier Ltd., 2015; *Vol. 132*.
(35) Kaur, H.; Carvalho, J.; Looso, M.; Singh, P.; Chennupati, R.; Preussner, J.; Günther, S.; Albarrán-Juárez, J.; Tischner, D.; Classen, S.; et al. Single-Cell Profiling Reveals Heterogeneity and Functional Patterning of GPCR Expression in the Vascular System. *Nat. Commun.* **2017**, *8*, No. 15700.
(36) Rajkumar, P.; Aisenberg, W. H.; Acres, O. W.; Protzko, R. J.; Pluznick, J. L. Identification and Characterization of Novel Renal Sensory Receptors. *PLoS One* **2014**, *9*, No. e111053.
(37) Mukherjee, S.; Sheng, W.; Michkov, A.; Sriram, K.; Sun, R.; Dvorkin-Gheva, A.; Insel, P. A.; Janssen, L. J. Prostaglandin E2 inhibits pro-fibrotic function of human pulmonary fibroblasts by disrupting Ca^{2+}-signaling. *Am. J. Physiol.: Lung Cell. Mol. Physiol.* **2019**, L810−L821.
(38) Zhao, S.; Fung-Leung, W. P.; Bittner, A.; Ngo, K.; Liu, X. Comparison of RNA-Seq and microarray in transcriptome profiling of activated T cells. *PloS One* **2014**, *9*, No. e78644.

DOI: 10.1021/acsomega.9b02811
ACS Omega 2019, 4, 17048−17059